

# The genesis of morphologies in extended radio sources: X-shapes, off-axis distortions and giant radio sources.

Lakshmi Saripalli & Ravi Subrahmanyan

*Raman Research Institute, C. V. Raman Avenue, Sadashivanagar, Bangalore 560080, India*

lsaripal@rri.res.in (LS), rsubrahm@rri.res.in (RS)

## ABSTRACT

We examine relationships between the morphology in double radio sources and the radio-optical position angle offset—the relative orientation of the radio axis with respect to the major axis of the host galaxy. The study was done for a representative sample of radio sources: the nearby (redshift  $z < 0.5$ ) 3CRR sources, and separately for samples of giant radio sources and X-shaped radio sources. We find that radio morphological features have a dependence on the radio-optical position angle offset and on whether the source is a major- or minor-axis source. The evidence indicates an anisotropic galaxy environment, related to the ellipticity of the host galaxy, that causes the source linear size evolution, strength of backflow in the radio lobes, off-axis lobe distortions and the formation of wings and X-shaped radio sources to depend on the radio-optical position angle offset. We identify a class of X-shaped radio sources, which are either edge-darkened or lacking hotspots, and appear to have inner doubles suggesting a restarting of activity. We suggest a common formation mechanism, requiring backflows, for these apparently FR-I X-shaped radio sources as well as the edge-brightened X-shaped sources.

*Subject headings:* galaxies: active — galaxies: elliptical — galaxies: halos — galaxies: jets — galaxies: structure — radio continuum: galaxies

## 1. Introduction

The extended radio morphologies in extragalactic radio sources manifest in a variety of structures. However, a basic double-lobed structure is invariably present and is accepted as fundamental to the nature of these radio sources. Among the various departures from this basic structure, radio galaxies with X-shaped morphologies have staked claim to the bizarre.

Apart from the usual double lobes, prototypical X-shaped radio sources have a second pair of lobes—sometimes larger than the main lobe pair—sharing the same radio core but oriented along a vastly different axis. Some of the most impressive examples of this class of X-shaped radio galaxies are 4C12.03, 3C223.1, 3C315 and 3C403 (Leahy & Perley 1991; Black et al. 1992; Leahy & Williams 1984).

Extended powerful radio sources typically has hotspots at the ends of the lobe pair, and diffuse emission extending from the hotspots towards the core, often forming a continuous bridge of relatively lower surface brightness. Leahy & Williams (1984) studied and classified distortions to normal bridge structures: they were found to be quite common, occurring in as many as 60% of sources, and the distortions occurred predominantly at the centres with either one or both lobes deflecting off the radio axis. These lobe deviations at the centres were suggested to be a consequence of interaction between the strong backflows and a gaseous halo associated with the host galaxy. Inversion symmetry in the central distortions involved backflow material encountering an asymmetrically distributed galaxy halo. The large deviations observed in X-shaped radio sources were suggested as resulting from a deflection of backflowing material into a cavity created by past activity along a very different direction.

Recent phenomenological studies of the extended emission associated with active galactic nuclei (AGN) have provided additional clues to the genesis of the radio morphologies. Capetti et al. (2002) presented evidence for a preference for X-shaped radio galaxies to be hosted by galaxies with relatively high ellipticities and for the lobe deflections to be oriented close to the host minor axes. Based on their findings a model for formation of X-shaped structures was preferred wherein backflows occurring closer to host major axes responded to the high cocoon pressure by escaping along the direction of maximum pressure gradient, which is along the host galaxy minor axis. While the latter finding of the ‘wings’ being preferentially along host minor axes has been subsequently confirmed, observational support for the stringent requirement for high host ellipticities has not been forthcoming (Springmann & Cheung 2007). Supporting this model, X-ray emission corresponding to a thermal gaseous halo has been detected in the host of an X-shaped radio source 3C403: the highly elliptic X-ray contours of the halo follow the elliptic galaxy isophotes and appear tangential to the sharp bend in the radio contours of the backflow, suggesting a deflection interaction (Kraft et al. 2005).

Saripalli et al. (2008) presented an interesting case of a giant, FR-I type (Fanaroff & Riley 1974) X-shaped radio galaxy that obeys the same empirical relations found by Capetti et al. (2002) for FR-II X-shaped sources. The discovery of its restarted nature via the finding of an inner, edge-brightened double source sharing the same core and radio axis suggests a model

consistent with the backflow scenario.

In an attempt to account for the Giant Metrewave Radio Telescope (GMRT) observations of anomalous spectral indices in the twin lobes, Lal & Rao (2007) proposed that the X-shapes originated in two closely spaced AGNs where each was associated with a pair of lobes whose radio axes are at a large angle with respect to each other.

On the other hand, considering the observational evidence for episodic activity associated with the AGNs in several radio sources (Roettiger et al. 1994; Subrahmanyan et al. 1996; Schoenmakers et al. 2000; Saripalli, Subrahmanyan & Udaya Shankar 2002, 2003; Saikia, Konar & K 2006), the obvious question is whether X-shaped radio sources are a result of a restarting of beams following a flip in the ejection axis (Leahy & Williams 1984; Zier & Biermann 2001; Merritt & Ekers 2002; Liu 2004). This alternative model—the binary black-hole merger model—suggests the eventual merger of two black holes, one of which is responsible for the radio jets, as causing a rapid flip in the spin axis resulting in a new double radio source along a very different axis. This is the preferred model for the multi-frequency observations of two X-shaped radio galaxies presented by Dennett-Thorpe et al. (2002), and for the double-peaked low-ionization emission lines observed by Zhang, Dultzin-Hacyan & Wang (2007) in an X-shaped source. The existence of wings that are larger than the main source extent has been viewed as an argument against the backflow model (Leahy & Parma 1992); such structures are accounted for in the black-hole merger model as relic emission from an independent past activity epoch, which may have been ongoing for longer time compared to the current activity. However, as has been pointed out by Kraft et al. (2005), it is possible, within the backflow model, for a very asymmetrical environment and fast backflows to result in wings advancing faster than the main lobe.

We take up the issue of the formation of X-shaped structures in this paper, expanding the discussion to the formation of off-axis deformations that are less spectacular, and including the question of formation of giant radio galaxies. We first discuss the place of FR-I X-shaped sources in Section 2. We then explore the relationships between the radio axis and host galaxy major axis for several samples, in Sections 3 to 6, representing different radio morphological structures. We find evidence that a variety of radio morphological features might be a result of interactions between the jets, backflows, and an asymmetric environment, and the discussion in Section 7 consolidates the viewpoint that the radio morphologies are related to whether the source is of the minor- or major-axis class, as defined by the relationship between the radio axis and optical axes.

At the outset we define an X-shaped source to be one that has extensions on either side of the core in addition to the main lobes, with at least one extension having a total extent more than 50% of the main lobe; such extensions are referred to herein as ‘wings’.

Extensions that are less than 50% of the corresponding lobes are called ‘mini-wings’. We adopt a flat cosmology with Hubble constant  $H_0 = 71 \text{ km sec}^{-1} \text{ Mpc}^{-1}$  and matter density parameter  $\Omega_m = 0.27$ .

## 2. Edge-darkened and hotspot-less X-shaped radio galaxies

X-shaped structures are almost always found in edge-brightened radio sources. This aspect has been an important clue to the cause of the X-shaped structures, and has been used to argue for or against models proposed for the formation of the X-structures.

In models that require backflows and invoke deflection of backflowing lobe material for the creation of the prominent wings, edge-brightened radio structures—indicative of powerful jets and compact hotspots—are necessary. In this class of models FR-I sources would not be expected to show X-shaped structures. On the other hand, the lack of FR-I X-shaped sources has been viewed as a puzzle or attributed to negligible interaction between the black hole binary and radiatively inefficient accretion disks in FR-Is (Dennett-Thorpe et al. 2002; Liu 2004). It has also been used as an argument against models in which the wings are relics of past activity, which was along a different position angle (Capetti et al. 2002).

This belief that X-shaped radio sources are exclusively edge-brightened and hot-spot radio galaxies—owing to the lack of observations of X structures in edge-darkened radio sources—has been dented by the recent discovery and imaging of the clearly FR-I X-shaped radio galaxy B2014–558 (Saripalli et al. 2008). Subsequently, we have carefully examined X-shaped radio galaxies in the literature and have identified several more examples, which have either edge-darkened lobes or edge-brightened lobes that lack hotspots. Examples of FR-I type edge-darkened X-shaped sources, or X-shaped sources lacking hotspots at the ends, are considered a clear argument against models that require backflows for the formation of the secondary radio axis. Since the sources we have identified have no hotspots at the ends of their lobes, backflows are not expected. Therefore, it would appear that their secondary radio axes could not have formed via the deflection of backflows, suggesting that X-shaped structures—at least in such cases—might form via flips in the radio ejection axis.

Below, we list and provide brief notes on the X-shaped radio galaxies that we have identified to have edge-darkened lobes, or lacking hotspots at their lobe ends. All of these have secondary radio structures or ‘wings’ that are at least 50% of the extent of the main radio axis.

(1) B2014–558: A study of the radio properties of this unusual FR-I X-shaped radio galaxy has been presented by Saripalli et al. (2008). To our knowledge, it is the first clearly

FR-I type X-shaped radio galaxy to be recognized as such and studied in detail. The source is atypical in more than one aspect. It is the only known giant radio source with the classic X-structure. As discovered by Saripalli et al. (2008), B2014–558 is also a double-double radio source and has an inner double at the centre, aligned with the 1.5-Mpc outer lobes, and nearly two orders of magnitude smaller in linear extent.

(2) 4C12.03: Although the radio source appears to have an edge-brightened morphology, the lobes do not possess compact hotspots at the ends (Leahy & Perley 1991). 4C12.03 has one of the most prominent set of wings among known X-shaped radio sources: the wings span an extent that is larger than that of the main radio axis. Once again, the radio source is of the double-double category and has an embedded inner double at the centre, with extent about 30 kpc, that is observed to be collinear with the main lobes.

(3) 3C315: This is a well studied X-shaped radio source (Leahy & Williams 1984) with clearly edge-darkened lobes, although the northern lobe has a warm-spot located somewhat away from the end. There are no compact hotspots in either of the two main lobes. Apart from the relaxed appearance for the lobes along the main axis and the lack of hot spots, which are unusual in X-shaped radio sources, 3C315 appears to possess a relatively small, inner edge-brightened double radio source at the centre as in the previous two cases presented above. The inner-double is about 8 kpc in extent and is closely aligned with the axis of the main source (3CRR Atlas<sup>1</sup>, eds. J. P. Leahy, A. H. Bridle, R. G. Strom).

(4) J0116–473: Saripalli, Subrahmanyan & Udaya Shankar (2002) presented a detailed study of this radio source, pointing out that it has a double-double structure and is a spectacular example of recurrent nuclear activity in which new edge-brightened inner lobes have been created embedded within outer edge-brightened relic lobes of past activity; the outer lobes lack hotspots. Additionally, they drew attention to a peculiar distinct bar-like feature that is associated with the inner part of the southern lobe and offset from the core, and is oriented almost orthogonal to the radio source axis. If we consider this bar as a ‘wing’ then J0116–473 is another example of a restarting X-shaped radio galaxy that lacks hotspots at the lobe ends.

(5) B1531+104: This source has been observed by Owen & Ledlow (1997) and is a radio source in an Abell cluster. The source has wings that are asymmetric in extent: the eastern wing is less than half the extent of the western wing. There are no hotspots in both of the main pair of lobes. As in previous examples listed above, B1531+104 is observed to have an inner double structure that constitutes all of the bright structure in the source and is aligned with the main axis as defined by the main pair of lobes.

---

<sup>1</sup><http://www.jb.man.ac.uk/atlas/>

(6) B1207+722: This source is also a member of an Abell cluster and was imaged by Owen & Ledlow (1997). The observations clearly show a pair of wings centered on the core. The two main lobes have their brightest regions well recessed from the lobe ends; this attribute is more manifest for the northern lobe.

(7) NGC 326: Radio images of this source have been presented by Murgia et al. (2001), and it has been noted that both of the pair of main lobes lack compact hotspots at their ends. The wings in NGC 326 are among the most spectacular of such structures: they are more than twice the main source in extent. The host is part of a dumb-bell galaxy pair.

(8) 3C76.1: This source has a clear edge-darkened morphology although a pair of warm-spots are present at the lobe ends (Macklin 1983). The source lacks the classic bright pair of jets; instead, it has a nested pair of emission peaks on either side of the core. The S-shaped morphology of the main axis suggests that the jet may have precessed over a small angle. The source has a wide wing that is centred on the host galaxy.

For each of the above eight sources we have measured the sky angle between the radio axis, as defined by the main pair of radio lobes, and the major axis of the host galaxy. This has been relatively error free in six cases (B2014–558, 4C12.03, 3C315, J0116–473, B1207+722 and 3C76.1) in which the host galaxy images are clearly non-circular. It is significant that in all of these six cases the radio axis is oriented close to the major axis of the host galaxy, and the relative angle between the radio axis and major axis of the host is within  $45^\circ$ . The sources have been selected based on the radio morphology, with no bias related to the host optical properties and, therefore, we believe that our result is a finding of a genuine propensity.

It is remarkable that all of the six X-shaped radio sources that lack hotspots at the ends—with some, additionally, having edge-darkened lobes—show the same alignment between the main radio axis and the major axis of the host galaxy as was reported by Capetti et al. (2002) for FR-II X-shaped radio sources. Moreover, in all six cases with clearly non-circular hosts, the wing-lobe pairs lie on the same side of their host galaxy major axis, suggesting that the wings are a result of interactions of backflow from the corresponding lobe and an asymmetric environment associated with the host galaxy. Although it may seem that the discovery of the above edge-darkened and hotspot-less X-shaped sources might be evidence against the backflow model for the creation of wings in at least this class of sources, the alignment of the main radio axis with the optical major axis in these cases as well indicates that there may be a unified model across X-shaped sources with and without hotspots.

A clue is our remarkable finding that the radio images of five of the eight sources listed above clearly show evidence for an inner double—they are double-double radio sources—and

are presumably undergoing a renewal of central engine activity with new edge-brightened lobes aligned with the main outer lobes. In this picture the main lobes in all these cases are relics of past activity, which would likely have been of edge-brightened hotspot type if the beams in the past activity were the same as that at the present. We are led to believe that the X-shaped radio sources of the edge-darkened type and those that lack hotspots in their relaxed lobes have relic main lobes, which were created by powerful beams in the past. The relic main lobes, together with the wings, might have been created in that previous activity phase, with the wings a consequence of interaction of backflows with the host galaxy environment as in the backflow model. If the backflow model is applicable for all X-shaped radio sources with and without hotspots, this would require that the large-scale radio structure in all hotspot-less X-shaped radio sources are relics of past activity that was in the form of hot-spot radio sources. Additionally, this hypothesis also suggests a conversion from edge-brightened to edge-darkened morphology when the central beams of hot-spot radio galaxies are turned off, at least in those cases where backflows are strong and the beams are directed along the major axis of the optical host.

It may be noted that none of the above sources, which are hotspot-less and edge-darkened X-shaped radio sources, have radio powers significantly below the FR-I/FR-II break, consistent with the hypothesis that they are actually relics of objects with hotspots.

### **3. Radio morphology and the radio-optical position-angle offset: the 3CRR sample**

Capetti et al. (2002) demonstrated that, as projected on the sky, FR-II X-shaped radio galaxies tend to have their main radio axis aligned closer to the major axis of the host elliptical galaxy. As we suggest in the previous section, X-shaped radio galaxies that lack hotspots and with FR-I type edge-darkened morphology do exist and also follow this trend. X-shaped radio galaxies are a small fraction of extended radio sources associated with AGNs, and it is of interest to examine whether subsets of the parent population, which exhibit other specific morphological features, also show similar preferences in the orientation of their main radio axis relative to the projected axes of the host, and whether relationships exist between morphological parameterizations and the radio-optical misalignment angle.

The results of several previous searches for correlations between the orientations of the radio axes and the host galaxy major or minor axes have been varied. Some early authors, for example, Sullivan & Sinn (1975), Gibson (1975) and Battistini et al. (1980), all failed to find any correlations. However, Palimaka et al. (1979) and Guthrie (1980) found a preference for the orientation of the radio axis along the host minor axis; moreover, the tendency for this

alignment was stronger for larger ( $> 176$  kpc) radio sources. Birkinshaw & Davies (1985) ruled out large misalignment angles ( $> 50^\circ$ ) between the radio axes and the minor axes of their hosts. Sansom et al. (1987) examined the radio-optical axis relations in a large sample of sources for which they obtained optical CCD images using the 1.5-m La Silla and radio images with the Very Large Array (VLA). They report a lack of any correlation of the radio axes with the projected optical axes as well as intrinsic stellar axes. More recently, the searches for correlations have been extended to examining for differences in correlations amongst subsets of the radio galaxy population: for example, Andreasyan & Sol (1999) find a greater preference for FR-II type radio sources to lie closer to the host minor axis, as compared to FR-I type sources, and the correlation was reported to be stronger for radio sources with higher axial ratios.

In this section, we revisit this issue by examining the 3CRR sample for relationships between radio morphological properties and the relative orientation ( $\Delta$ PA) between the radio axis and projected major axis of the host elliptical. This sample has the advantage of systematic, precision HST observations with uniform quality, as well as exhaustive radio observations available in the literature. We used the 3CRR sub-sample (Laing, Riley & Longair 1983) that included only the nearby ( $z < 0.5$ ) radio sources (the so-called ATLAS sample of J. P. Leahy, A. H. Bridle and R. G. Strom). These sources have been observed at radio wavelengths with high sensitivity to extended low-surface brightness components and the sample is well suited for examining for preferences in  $\Delta$ PA related to radio morphology.

The radio axes were measured from FITS images available in the 3CRR ATLAS website, using detections of core, hotspots and jets to define the radio position angle (P.A.). The orientation of the projected major axes of the optical hosts were taken primarily from the tabulations in de Koff et al. (1996) and Martel et al. (1999), who have derived the P.A. from HST images. In all cases we also examined their optical images by eye and if the tabulated value and the apparent P.A. of the optical image appeared inconsistent, or if a source was not included in the tabulations, we (i) used the 1.6- $\mu$ m FITS images downloaded from the HST archives, where available, and measured the P.A. of the elliptical isophotes, and (ii) in certain cases we used the FITS images from the digitized sky survey or 2MASS survey repository. In each case we also cross-checked against the body of observational results cited in the literature for consistency; a most useful reference work was the HST observations reported by Madrid et al. (2006) and the Issac-Newton Telescope (INT) data of Roche & Eales (2000). The P.A. and ellipticity values adopted for each galaxy refer to the largest scale structure in the optical images; a similar approach was adopted by de Koff et al. (1996) for their tabulations. The measurements were based on isophotes that were well above noise and mostly on linear scales of several kiloparsec. The P.A. from independent observations and images and using different data, where available, were found to be consistent and usually

within  $10^\circ$ . In cases where isophotal twists confused the issue, we adopted determinations based on the outer isophotes of HST archival images. The basic data used in the analysis presented herein is in Table 1.

In Fig. 1 we show the distribution of  $\Delta\text{PA}$  for the whole sample of 3CRR FR-II sources. The sources are distributed over the range  $0\text{--}90^\circ$  in their orientations relative to the host major axes and appear to show no preference for orientation closer to the host major or minor axis. This is similar to that reported by several previous studies (using ground based data prior to the HST).

Considering only the 61 3CRR FR-II radio galaxies, the median linear size is 284 kpc and the median P.A. offset of the radio axis from the optical major axis is  $46^\circ$ . Fig. 2 shows the plot of median projected linear size of the 3CRR FR-II sources binned in intervals of  $\Delta\text{PA}$ . The median linear size appears to increase systematically with radio-optical P.A. Sources with radio P.A. within  $45^\circ$  of the optical major axis have median linear size  $164 \pm 69$  kpc, whereas the sources with radio P.A. more than  $45^\circ$  away from the optical major axis have median linear size of  $314 \pm 39$  kpc; the errors in the medians have been determined here, as well as hereinafter, using the Efron Bootstrap method. We have compared the distributions of the linear sizes of the major axis sources ( $\Delta\text{PA} > 45^\circ$ ) with the linear sizes of the minor axis sources ( $\Delta\text{PA} < 45^\circ$ ) using the non-parametric Wilcoxon-Mann-Whitney test. The probability that the major axis sources could have a chance distribution in linear sizes as small as that observed is 6.5%, suggesting that the two distributions are genuinely different: the population of minor-axis sources have larger linear sizes as compared to the population of major-axis sources. It is interesting that when the sample is binned in  $22.5^\circ$  ranges, the bin containing sources with radio axes within  $22.5^\circ$  of the minor axis stands out with 4 giant radio galaxies with linear size exceeding 700 kpc, whereas the remaining three bins do not contain more than two giant sources each. The Binomial probability of obtaining four or more giants, of the total of 7 giants in the sample, by chance is 7% suggesting that our finding of a preference for giant radio sources to lie close to the host minor axis may be genuine. Such a minor-axis preference for giant radio galaxies was reported in earlier studies of Palimaka et al. (1979) and Guthrie (1980).

Interestingly, although not large in projected linear size, all the three Relaxed-Double radio sources in the 3CRR sample (3C310, 3C314.1 and 3C386) have radio axes within  $22.5^\circ$  of the minor axis; they are all less than about 400 kpc in size.

The sample of 3CRR radio galaxies with FR-II morphological classification, has 10 giant radio sources with projected linear size exceeding 700 kpc (3C33.1, 3C35, 3C46, 3C223, 3C236, 3C274.1, 3C326, 3C457, 4C73.08, DA240). Of these ten, two have host galaxies with circular shapes (3C46 and 3C274.1) and for one source (3C457) we could not locate useful

optical images in the literature or repositories. The remaining seven giant radio sources, for which the radio-optical P.A. may be reliably measured, have a median P.A. offset between the radio axis and the host minor axis of  $18^\circ$  (the one standard deviation upper limit to this offset is  $38^\circ$ ). Four out of the seven giant radio sources have their radio axes within  $20^\circ$  of the host minor axis, and an interesting aspect of the radio morphologies of these large radio galaxies is the complete absence of ‘winged’ structures; we will return to this point later below. The 3CRR FR-II sources, with linear sizes below 700 kpc, have a median offset of  $43^\circ \pm 9^\circ$  from the major axis.

It appears that jets in larger radio sources are observed to be preferentially oriented closer to the minor axis of the hosts; additionally, sources close to the minor axes of elliptical galaxies tend to have larger linear sizes. Radio jets may be uniformly distributed in radio-optical P.A. offset; however, it appears that radio jets that propagate closer to the host minor axis result in larger radio sources as compared to jets that emerge closer to the host major axis.

We identified 13 3CRR radio galaxies—including FR-I and FR-II type—that show prominent wing-like distortions in their lobes in the vicinity of the core (3C20, 3C28, 3C61.1, 3C76.1, 3C192, 3C285, 3C288, 3C315, 3C401, 3C433, 3C438, 4C12.03 and 4C73.08). Eight have wing distortions in both the lobes whereas five show a winged distortion in just one of the lobes. Only one source, 3C28, has mirror symmetric wings in which both the wing distortions are towards the same side of the radio axis. The median radio-optical P.A. offset,  $\Delta\text{PA}$ , for the 10 sources in this sub-sample that have clearly elliptical hosts was found to be  $22^\circ \pm 7^\circ$ . The median linear size of the sub-sample consisting of the 13 winged 3CRR sources is  $155 \pm 82$  kpc, which is significantly smaller than the median linear size of  $294 \pm 41$  kpc for the entire 3CRR sample. The largest source in this sub-sample is the giant radio galaxy 4C73.08, and the second largest is 4C12.03, both have  $\Delta\text{PA}$  in the range  $40\text{--}46^\circ$ . Of the remaining 11 sources in the sub-sample 8 have estimates for  $\Delta\text{PA}$ , and seven of these have  $\Delta\text{PA}$  less than  $30^\circ$ .

The indication is that radio galaxies with prominent lobe distortions in the form of wings are preferentially oriented closer to the host major axis, as is the case for X-shaped radio sources, and such sources are also relatively smaller in linear size. The above analysis indicates that winged distortions are relatively uncommon, and perhaps do not form, in giant radio sources and when the jets are closer to the minor axes.

We may draw particular attention to 3C433, which is one among the thirteen 3CRR sources with prominent wings. The source has wings in both lobes, but only one wing is close to the host galaxy. While the southern lobe extends west close to the location of the host, the extension in the northern lobe towards east occurs well away from the host. The

radio axis is close to the major axis of the host:  $\Delta\text{PA}$  is just  $20^\circ$ . Examination of the optical field shows a close neighbour at the location where the wing associated with the northern lobe appears to deflect east. The coincidence between the bend in radio structure and sky location of the companion galaxy is suggestive of a model wherein the backflow from the northern lobe is deflected by a gaseous halo associated with the neighbouring galaxy.

If sources with prominent wings in their lobes are preferentially oriented close to their host major axes, it is of interest to examine the morphologies of radio sources that are, instead, oriented close to their host minor axis. We formed a sub-sample of 13 3CRR FR-II radio sources (3C35, 3C79, 3C153, 3C219, 3C223, 3C236, 3C244.1, 3C303, 3C310, 3C319, 3C326, 3C390.3, 3C442A) consisting of all sources oriented within  $\pm 25^\circ$  of their host galaxy minor axis. The median linear size of these minor-axis sources is  $346 \pm 141$  kpc. Remarkably, only two among these 13 sources (3C310, 3C442A) have winged structures associated with their lobes. Nine sources (3C35, 3C79, 3C219, 3C223, 3C244.1, 3C303, 3C310, 3C319 and 3C390.3) have continuous bridges—the lobes extend all the way to the cores on both sides—and two of the sources (3C153 and 3C442A) have filled lobe emission on one side. Wing-type distortions are absent in all except two among these filled lobes. This sample of minor-axis radio sources includes five giant radio sources. This examination of the sub-sample of 13 minor-axis sources that have radio axes aligned close to their host minor axes reveals that most are devoid of wings—including any scaled down manifestations of wing distortions or mini-wings—in their lobes.

We may also examine the morphologies of radio galaxies selected to have radio axes close to their host major axes. Sixteen FR-II-type radio galaxies (3C67, 3C200, 3C28, 3C436, 3C173.1, 3C401, 3C268.3, 3C299, 3C61.1, 3C33.1, 3C433, DA240, 3C388, 3C42, 3C300 and 3C123) were identified in the 3CRR sample, which have radio axes within  $\pm 25^\circ$  of their host major axes. The median linear size of this major-axis source sample is just  $149 \pm 63$  kpc. Half of the sources have mini-wings, wings or plume structures associated with their lobes and five (3C28, 3C401, 3C61.1, 3C433 and 3C123) of these eight display prominent wings. However, it may be noted that some of these major-axis sources have no wings (3C436, 3C173.1 and 3C33.1) and some have large emissions gaps between their cores and lobes (3C299, 3C268.3 and 3C67). There is only one giant radio galaxy, DA240, in this restricted sample; although DA240 does not have lobe distortions such as wings or mini-wings, both its lobes have unusually small axial ratios (ratio of the lobe extent along the radio axis, from core to the end, to the transverse width of the lobe), and are individually nearly circular in morphology.

To conclude this section, there appears to be two classes of radio galaxies: major-axis and minor-axis sources that have differing radio structures and different median linear

sizes. Most major-axis sources have relatively smaller extents and often exhibit off-axis lobe distortions; minor-axis sources appear to have relatively larger linear sizes and lack off-axis wing distortions in their lobes.

#### 4. Radio morphology and the radio-optical position-angle offset: the Giant Radio Galaxy sample

In this section we explore the radio-optical P.A. offsets in the 1-Jy sample of giant radio galaxies of Schoenmakers et al. (2000), restricting to the sub-sample of redshift  $z < 0.15$  objects for which optical images that have sufficient quality for the reliable determination of P.A.s exist. The sub-sample consists of 17 giant radio galaxies (GRGs) with projected sizes exceeding 700 kpc; five of these are members of the 3CRR sample. The methodology adopted for estimating the radio and optical P.A.s was the same as for the 3CRR sample. Three sources (B0050+402, B0658+490 and B2147+816) had poor optical images and were rejected; of the remainder, one host galaxy (B1309+412) had a shape close to circular and was also omitted for the analyses that required  $\Delta$ PAs.

We derive a median offset of  $11^\circ \pm 3^\circ$  between the radio axis and host minor axis for the reduced sample of 13 GRGs with  $z < 0.15$  and size  $> 700$  kpc; as many as 11 of the 13 have radio axis within  $30^\circ$  of the host minor axis. The median radio-optical P.A. offset for the 3CRR giant radio galaxies (with size  $> 700$  kpc) is consistent, within errors, with the value obtained for this GRG sample; additionally, it may be noted that the omission of the five 3CRR giants from this GRG sample does not change the computed median.

The analysis of the 3CRR sample indicated that relatively few GRGs manifested large wings. To explore this issue for a larger sample, we combined complete samples of GRGs with good radio images: the 11 3CRR giants, 24 giants from the 1-Jy sample of Schoenmakers et al. (2000) (excluding B0050+402 for which a good radio image could not be found in the literature), 7 giants from the sample of Subrahmanyan et al. (1996) (excluding B2356–611 that has a linear size  $< 700$  kpc) and the SUMSS sample of 16 giant radio galaxies from Saripalli et al. (2005). It may be noted here that the 11 3CRR sources and the 7 sources in Subrahmanyan et al. (1996) were well-imaged; additionally, the sources in Schoenmakers et al. (2000) and Saripalli et al. (2005) are from surveys, with high surface-brightness-sensitivity, at 327 MHz and 843 MHz respectively. Avoiding repetitions, we have 52 GRGs in all with linear size  $> 700$  kpc. We examined their radio images for off-axis lobe distortions close to the centre: off-axis plumes with extent  $> 50\%$  of the associated lobes are referred to herein as ‘wings’; those  $< 50\%$  of their associated lobes are referred to as ‘mini-wings’.

A large fraction (87%) of the giant radio galaxies in this compilation do not have wings. Only 3 (4C73.08, B0114–476 and B0511–305) of the 52 have extensions resembling wings, and in all of these sources the wings are in only one of the pair of lobes. One source, 3C46, has a pair of mini-wings and another three (3C274.1, B0211–471 and B1545–321) have mini-wings on only one side. Clearly wings of the kinds seen in X-shaped radio galaxies are not present. If we restrict to only the 18 well-imaged sources—the 3CRR giants and those in the compilation of Subrahmanyan et al. (1996)—we find that 11 do not have wings, 3 have wings (only in one lobe), 3 have mini-wings (only in one lobe) and one has a pair of mini-wings, confirming the relative paucity of wings in GRGs that was inferred for the larger compilation.

To examine the relationship between the radio axes and host optical axes for a larger sample of GRGs, we used the combined sample, but restricted to sources for which relatively good optical data is available: (a) the 11 3CRR GRG hosts for 10 of which HST images are available, (b) an additional 9 sources in the Schoenmakers et al. (2000) sample of nearby  $z < 0.15$  1-Jy giants (excluding the 5 common to 3CRR), for which sufficiently good DSS or 2MASS images were available, and (c) 4 of the 7 GRGs from the Subrahmanyan et al. (1996) sample for which Anglo-Australian Telescope (AAT) imaging observations or SuperCOSMOS digitized images with sufficient quality were available. Our measurements were checked against images and notes from various publications in the literature. In all there were 24 sources: Table 2 lists the members from the  $z < 0.15$  1-Jy Schoenmakers et al. (2000) sample (including the 5 common to 3CRR) and the 4 from Subrahmanyan et al. (1996) sample; the six members that are part of the 3CRR nearby sample are in Table 1. Five GRGs (3C46, 3C274.1, B0511–305, B1545–321 and B1309+412) were associated with hosts with apparently circular images and one (3C457) had only a poor optical image and, consequently, host P.A.s could not be reliably estimated for these.

Fig. 3 shows the histogram of the  $\Delta$ PA distribution for the 18 GRGs with non-circular hosts and for which optical-axis P.A.s could be determined; a clear preference for minor axis orientation is seen. Among these 18 GRGs, 12 have radio axes within  $30^\circ$  of the host minor axes whereas 6 have radio axes more than  $30^\circ$  from the host minor axes. The chance probability that 12 or more of the 18 giants have radio axes within  $30^\circ$  of the host minor axis is as low as 0.4% if they were uniformly distributed. The median P.A. offset between the radio axis and host minor axis for the 18 GRGs, for which optical host P.A.s could be reliably measured, is  $11^\circ \pm 9^\circ$ . This median offset is similar to that obtained for the 3CRR giants, and separately for the 13 Schoenmakers et al. (2000) giants.

We may compare the radio morphologies of two groups of giant radio galaxies—those with radio axes within  $30^\circ$  of the host minor axis and those with larger offsets. All the 12

GRGs with radio axis close to the host minor axis lack central extensions: both wings and mini-wings. Several of these GRGs show emission gaps; what is noteworthy is that in every case where the lobe emission extends all the way to the central core no wings or mini-wings are apparent in the radio images (e.g. 3C35, 3C223 and B0309+411). In the 6 GRGs with radio axis more than  $30^\circ$  offset from the host minor axis, winged lobes are manifest in 4. 4C73.08 and B0114–476 have wings in one lobe each and B0211–479 and DA340 have a mini-wing each.

To summarize this section on GRGs, examination of the radio morphologies and comparison with P.A.s of their optical host galaxies shows that a significant fraction of GRG radio axes are close to the optical minor axes and that these minor-axis GRGs are relatively deficient in lobe distortions in the form of wings and mini-wings. The few GRGs with radio axes oriented away from the minor axes of their hosts are relatively abundant in extended wings and mini-wings.

## 5. Radio morphology and the radio-optical position-angle offset: X-shaped radio sources

In this section the distribution of radio-optical P.A. offsets in X-shaped radio sources are examined and relationships between the source morphology and radio-optical P.A. offset are studied. A total of 31 X-shaped radio sources have been compiled from the literature. Selection criteria adopted were: (a) presence of off-axis lobe distortions at the end of the lobe closer to the core, which exceed 50% of the length of the associated lobe, (b) the distortion ought to be asymmetric with respect to the main source axis, and (c) the off-axis distortion must be present in at least one of the lobes in the pair. These criteria exclude the numerous sources with mini-wings. To the list of known X-shaped radio sources compiled by Cheung (2007) (see his Table 1) we added sources from the 3CRR sample and from the Abell clusters imaged by Owen & Ledlow (1997), which were recognized as satisfying the criteria for X-shaped structure. There are two quasars in the compilation. The total radio powers span a wide range from  $3 \times 10^{24}$  to  $10^{27}$  W Hz<sup>-1</sup>. Our sample is more than three times larger than the sample used by Capetti et al. (2002) in their study of the distribution in radio-optical P.A. offset.

X-shaped radio galaxies are believed to be exclusively associated with FR-II type radio sources (Capetti et al. 2002). However, in our compilation of 31 sources we identify as many as 8 that are either edge-darkened or lack hotspots at the lobe ends despite being edge-brightened. All have been described above in Section 2 along with a discussion on the implications for the backflow model for X-shaped radio sources.

In Table 3 we list parameters for our sample of X-shaped radio sources. For deriving the P.A.s of the main radio axis we adopted the same method we used—and described above—for the 3CRR sources. For obtaining P.A.s for the optical hosts: in the case of 3CRR sources we used the values derived above; for the remaining sources the optical P.A.s were measured on the DSS or SuperCOSMOS images at a surface brightness level at least three times above rms noise. We expect measurement errors to be less than  $10^\circ$ . For measurement of P.A. of the radio wings we mostly used the P.A. of the central ridge line of individual wings. The wings in a pair of lobes are usually parallel, although the wings are often not collinear; in a few cases (3C315 and 3C403) we adopted the mean P.A. for the two wings and in cases where only one wing was well defined its P.A. was used.

Fig. 4, which shows the distribution in P.A. of the main radio axes and wings for our sample, reveals that the main radio axes in X-shaped radio sources are all oriented within  $50^\circ$  of their host major axis with median offset of  $25^\circ \pm 6^\circ$ . The Fig. 4 also shows the different distributions in the P.A. offsets for the wings compared to the main radio axes: whereas the main radio axes are fairly uniformly distributed over offsets in the range  $0\text{--}50^\circ$  of the host major axes, and only two sources have main radio axes within  $10^\circ$  of the host major axes, the wings are preferentially close to the host minor axes and as many as 8 have wings within  $10^\circ$  of their host minor axis. The probability that the different distributions for the orientations of the main sources and the wings occurs by chance is  $< 0.01\%$  based on the Wilcoxon-Mann-Whitney test. If we exclude the two quasars and sources with faint or unidentified or circular host galaxies, we have 10 sources whose wings are within  $10^\circ$  of the minor axis of their hosts and 9 sources with wings making larger angles. These distributions imply that although the main radio axis might be somewhat offset from the host major axis, the wings tend to align along the host minor axis. These confirm the work of Capetti et al. (2002).

Fig. 5 shows a plot of the ratio of projected extents of wing to main source versus source size. The two quasars (4C01.30 and J2347+0852) have large wings relative to their main radio axes, as would be expected because their main radio axes would be foreshortened by projection effects. Considering the radio galaxies in the sample, the median projected wing-to-main-lobe ratio shows no evidence for a trend with projected linear size: the median value of this ratio is  $0.91 \pm 0.05$ . The distribution over this ratio appears to have a long tail towards large values of the wing-to-main-lobe ratio. Fig. 5 suggests that sources with relatively larger projected linear size, including giant radio sources, are lacking in examples of sources with large wing-to-main-lobe ratio. Such a trend is consistent with a picture wherein asymmetry in galaxy environment results in larger sources being minor-axis sources with poorer backflows and off-axis distortions in their lobes. However, because of the small size of the sample it is difficult to correct for projection effects, which may be partly responsible

for this trend.

The scatter plot in Fig. 6, showing the distribution in radio power versus the P.A. of the wings relative to the major axis of the host, is indicative of a weak link between the orientation of the wings with respect to the host major axis and the source total radio power (correlation coefficient between the wing position angle and the logarithm of the total radio power is 0.55). The X-shaped radio sources in which the wings are well away from the host minor axis are the ones with relatively lower total radio power, and the more powerful X-shaped radio sources tend to have wings along the host minor axes. Although their main radio axes might make angles of as much as  $50^\circ$  to the host major axes, as is the case for 4C12.03, 3C403 and B2356–611, these powerful sources continue to have minor axis wings.

In Fig. 7 we show the distribution of the ellipticity of the host galaxies of X-shaped sources compared to that for 3CRR FR II hosts. The hosts of the X-shaped sources appear in the plot to have a distribution to greater ellipticities and the median ellipticity for the hosts of X-shaped sources is  $0.28 \pm 0.05$ , which is somewhat greater than the median ellipticity ( $0.21 \pm 0.03$ ) of the hosts of 3CRR FR II radio sources. The indications here are in agreement with an earlier suggestion (Capetti et al. 2002) of relatively higher ellipticity for the hosts of X-shaped sources. However, it may be noted here that this finding is not statistically significant since the Wilcoxon-Mann-Whitney test suggests a 26% probability that the observed distribution to higher ellipticities is a chance occurrence. As pointed out by Springmann & Cheung (2007), X-shaped radio galaxy hosts need not be highly elliptical relative to the parent population of hosts of radio galaxies. In our sample there are 6 sources with apparently circular host galaxies. As galaxy ellipticity is known to vary with radius we need a more quantitative measure for this parameter, and high quality images of a sample of hosts, to examine for correlations with more confidence.

## 6. Central lobe extensions as mini wings?

We have also examined the radio-optical axis offsets in radio sources with mini-wings: inversion-symmetric central distortions that result in extensions of the lobes transverse to the main radio axis, which have lengths less than half the length of their respective main lobes. Our sample of mini-wing sources consists of 11 members of the 3CRR sample: 3C19, 3C33, 3C42, 3C46, 3C234, 3C274.1, 3C284, 3C319, 3C341, 3C300 and 3C381. Because the P.A.s of the mini wings are ill defined, we examined only the radio-optical P.A. offsets of main lobes with respect to the optical axes.

Five of the host galaxies appear circular, in 2 sources (3C42 and 3C300) the radio

axis is within  $25^\circ$  of the host major axis, and in 4 (3C33, 3C284, 3C319 and 3C381) the radio axes make angles exceeding  $50^\circ$  relative to their host major axes. We examined the four cases of large offsets individually. In two sources, 3C284 and 3C381, the P.A. offset between the radio axes and extended emission-line gas is about  $35^\circ$  and  $30^\circ$  respectively (McCarthy, Spinrad & van Breugel 1995). It is remarkable that the lobe deflections resulting in mini wings appear to occur near the boundary of the emission line gas distribution and the directions of apparent bending are consistent with a deflection of backflow at the boundary. In the case of 3C319 the radio axis is close to the minor axis ( $\Delta\text{PA} = 78^\circ$ ): in this case the mini-wing is observed in only one lobe and here we identify a galaxy to the south of the host which appears to have deflected the backflow (Keel & Martini 1995). In the fourth case, 3C33, extended emission line gas at P.A. of about  $20^\circ$  with respect to the southern lobe appears to be influencing the backflow and deflecting it East, whereas the northern lobe deflects East somewhat away from the core (Baum et al. 1988). A member of this sample, 3C341, is noted to have a circular galaxy image: emission-line gas is observed to be extended over 32 kpc and oriented nearly North-South and the relative angle between the radio axis and the gas major axis is about  $50^\circ$  (McCarthy, Spinrad & van Breugel 1995). To summarize, in these mini-winged sources the P.A. of the emission-line gas distribution appears to replace the role of the host galaxy in the shaping of the backflows.

## 7. Summary and discussion

The problem for the backflow model posed by the discovery of a class of X-shaped radio sources with edge-darkened lobes and lobes that lack hotspots is alleviated by the discovery of double-double morphologies in a relatively large fraction of them, which suggests that these X-shaped radio sources appear so only because their central engines have recently ceased feeding their outer lobes. Excluding the two with circular hosts, all the six sources we have identified as belonging to this class have their main radio axes closer to the host major axis and wings that are closer to the host minor axis—properties associated with FR-II X-shaped sources. Moreover, the lobe-wing pairs are observed to be on the same side of the major axis, as required by the backflow model for the formation of X-structures. Therefore, it appears that whether of FR-I type or FR-II type the backflow model is able to explain the formation of wings in these sources. The inference that X-shaped sources that appear to have an FR-I structure were FR-II type hot-spot radio sources in the past active phase, with strong backflows that interacted with the host galaxy, leads to the suggestion that the edge-brightened FR-II lobes transformed to edge-darkened FR-I morphology with time following the cessation of jets, at least for these major-axis sources with strong backflows.

For the 3CRR sample of nearby radio sources we have shown that there is no preferred orientation of the radio axis: radio galaxies emerge at all angles with respect to the host major axis. This lack of a preferred orientation for a general population of radio galaxies was also the conclusion of several previous investigations (Sansom et al. (1987) and references therein). However, examining the properties of large-scale radio structures in the nearby 3CRR powerful radio galaxies, clear differences are seen depending on the direction of propagation of their jets relative to their host axes. Sources that are oriented along a direction closer to the host major axis—the major-axis sources—do not grow large on average and tend to be associated with winged lobe structures. In contrast, minor-axis sources have larger projected linear sizes on the average and rarely develop off-axis distortions in their lobes.

Separately, for a sample of giant radio galaxies, we have shown that there is a strong preference for the radio axis to be along the host minor axis: giant radio sources are predominantly minor-axis sources. While a small fraction do form along directions closer to the host major axes these are found to have prominent off-axis lobe structures. Once again, similar to the 3CRR sample, major-axis giant radio sources are found to be associated with winged structures.

For our sample of 31 X-shaped sources, which is larger than the sample examined by Capetti et al. (2002), we find a striking preference for the main radio axes to be in the quadrants of the host major axes, and for the wings to be in the quadrants containing the host minor axes; this is consistent with and an improvement on the significance of the earlier work.

### **7.1. Asymmetry in galaxy environment: influence on forward and backflows**

Several previous studies demonstrated a link between environment and radio structures: McCarthy, van Breugel & Kapahi (1991) presented the correlated asymmetries between radio source extents and extended emission-line gas distribution, and Saripalli et al. (1986) and Subrahmanyam et al. (2008) for correlated asymmetries between radio source extents and ambient large-scale environments of giant radio galaxies. That the ambient medium affects radio morphologies is also demonstrated by examples like 3C433 and NGC 326, in which the lobes on the side of the close galaxy neighbour develop off-axis deviations correspondingly earlier, and examples like 3C341 and 3C28, in which the extended emission-line region appears to shape and redirect plasma flows although influence of an overdensity of hot, X-ray emitting gas, particularly in 3C28, may have a greater influence (e.g., Hardcastle et al. (2007), Evans et al. (2008)). In all of these examples it is thermal gas concentrations that

are encountered by radio jets or bulk synchrotron plasma flows, resulting in a hindrance to the forward flow or a deflection of backflows. Our findings of a clear connection between the morphological properties of powerful radio galaxies and their orientation relative to their host—whether the radio source is a minor- or major-axis source—is suggestive of an influence of asymmetry in the host galaxy environment on the radio source morphology. The previous case studies and findings of circumstantial evidence for interactions between radio synchrotron plasma and thermal gas suggest that our work presented herein may be interpreted as arising due to differences in the ambient density and gradients thereof along the host galaxy major axis compared to that along the host galaxy minor axis. These differences may differentially affect the forward propagation of jets in the major and minor axis directions and the strength of backflows; additionally, the off-axis deflection of backflows would themselves differ between minor- and major-axis sources owing to the different strengths in the backflows and pressure gradients.

It may be noted here that although ‘mini-wing’ type lobe distortions have been associated with thermal gas concentrations in the form of extended emission line regions, the more spectacular ‘wings’ in X-shaped radio sources appear to be a consequence of lobe interactions with the more extensive thermal halos of galaxies.

Since double radio sources are observed to have similar axial ratios independent of linear size (Subrahmanyan et al. 1996), it follows that backflow—at least of the relativistic electrons—is essential if the bridge is to remain visible despite the inevitable expansion losses. Studies have indicated that backflowing plasma from hotspots in powerful radio galaxies might attain quite high velocities: perhaps as much as several tenth’s of the velocity of light (Alexander & Leahy 1987). The conditions encountered by the backflowing plasma in the vicinity of the host galaxy in the two cases of major- and minor-axis jet propagation are different. Assuming that the gaseous environment of the host galaxy has the ellipticity and P.A. of the stellar component, the gas density and pressure gradients would be greater along the minor as compared to the major axis.

## 7.2. Clues from the ‘wings’ in double radio sources

In most winged radio sources and the X-shaped radio sources an association in the form of a connectedness in structure is often observed between the wing pair and the lobe pair: each of the wings are associated with particular lobes and in many it has been observed that the associated wing and lobe are on the same side of the host major axis. The connection between lobe and associated wing has sometimes also been observed in a continuity in B-field. These argue in favor of models in which wings are fed by backflows from lobes.

It is remarkable that wings are observed exclusively in sources that have continuous or filled main lobes: there is no case in which the main lobes are docked and a pair or wings are observed as a symmetric structure extending across the core, disconnected from the main lobes, and forming a secondary pair of lobes orthogonal to the main lobes. Sources with continuous bridges are expected to be those with strong backflows and, therefore, this finding underlines the importance of backflows, and the channeling of backflows into wing structures, for the existence of visible wings.

Mechanisms suggested for the backflow deflection have been either a buoyant lifting of the plasma away from the dense thermal galactic halo gas or a force provided by an overpressured cocoon of synchrotron plasma that then seeks the direction of the steepest pressure gradient along the minor axis. The wings are often observed to have rather collimated morphologies with magnetic field mostly along the linear extent. The integrity of the deflected backflow may not be maintained if it were to just expand freely; therefore, while buoyancy may be playing a role, a driving force is required. An overpressured cocoon as suggested by Capetti et al. (2002) is a possibility, although rather than originating only at the ends of the lobes it may be that the overpressure develops naturally as the backflow stalls upon reaching the denser regions of the galactic halo. Collimation in the main lobes is thought of as arising due to greater advance speeds at the ends of the lobes compared to the lateral expansion speeds of the sides of the lobes. Collimation in the wing structures may arise for a similar reason: within the backflow model and in an asymmetric environment the wings advance most rapidly along the direction of steepest pressure and density gradient. Since the steepest gradient is along the minor axis of the host galaxy, then this might also be the preferred direction for the orientation of the wings, consistent with the finding in Fig. 4.

As noted earlier in Section 5, the median ratio of wing to lobe lengths is 0.91 for X-shaped sources, implying that there are as many X-shaped sources with this ratio exceeding 0.91 as those with this ratio in the range 0.5–0.91. The suggestion that large wing-to-main-lobe ratios are seen only in relatively smaller radio sources, and that this ratio decreases with increasing source size, is consistent with evolution of radio sources in an anisotropic environment, which manifests in a retardation in the growth of major-axis sources, enhancement in their backflows, and formation of wings of length dependent on the strength of the backflows and the retardation of the forward advance of the jets.

Within the backflow scenario it is possible for extreme asymmetry in the environment to result in wings advancing faster than the main lobe, resulting in wings larger than the main lobe extent. This would require the main lobes to be directed along the direction of greater density, and the backflow creating wings along the direction of lower density. Assuming that the heads at the ends of the main lobes as well as the advancing ends of the wings are ram

pressure limited in their speeds by the external density, the ratio of the external densities encountered by the main lobes and wings would have to exceed the ratio of the pressures in the heads and wings. Such an explanation for X-shaped radio sources in which the wings are larger than the main source extent weakens the argument that the existence of such structures requires axis flips for their origin.

Concerning the wings in X-shaped radio sources, we may list three findings that argue in favor of a pre-existing channel along the minor axes or a preferred plane normal to the major axes as a conduit for the backflowing material: (1) the collimation observed in many wings of X-shaped radio sources, (2) the larger extents observed for many wings compared to the main lobes, and (3) the finding, as shown in Fig. 4, that wings tend to align close to the minor axes of the hosts even though the main radio axes have a wider spread in distribution about the major axes. Our discussions above suggest that these findings may indeed have explanations within the backflow model, indicating that a purely environmental explanation is possible.

### 7.3. The black-hole merger model

First, it may be noted that ‘dead’ radio galaxies are known to be notoriously rare (Blundell & Rawlings 2000). Once the jets cease feeding the lobes, they are expected to suffer severe adiabatic expansion losses and disappear over a relatively short timescale compared to source lifetimes. In this context, it is difficult to understand the wings of X-shaped radio sources as relics of past activity when the renewed activity following a jet-reorientation has evolved to a linear size exceeding that of the wing, and particularly in the case of giant X-shaped radio sources.

Second, the morphologies of wings in X-shaped radio sources bear little resemblance to the known relic double radio sources like IC2476 (Cordey 1987) and SGRS J1911–7048 (Saripalli et al. 2005), both of which have an overall edge-brightened and bounded appearance. It is perhaps more appropriate to compare the wings with relics that have been ‘dead’ for timescales similar to that in which axis flips might occur: this has been estimated to be about  $10^7$  yr (Merritt & Ekers 2002). The outer relic lobes of double-double radio galaxies, which are believed to be restarting, have been estimated to have been ‘dead’ for such timescales (Schoenmakers et al. 2000; Saripalli, Subrahmanyan & Udaya Shankar 2002; Safouris et al. 2008); however, none of the wings in X-shaped radio sources resemble these relics. Unlike the range of morphologies observed for the general population of radio galaxies, all winged structures appear to be continuous and well filled with no emission gaps towards their central regions. It is unlikely that axis flips would occur only in a narrow range of

source morphologies.

The indications are that it is unlikely that X-shaped radio sources represent a pair of relic lobes and another independent pair of lobes created following an axis flip. In this context, it is of interest to consider the model proposed by Lal & Rao (2007), wherein the twin lobes are thought of as separate radio sources associated with a close pair of AGNs. A compelling argument against such a model is that the morphologies of the main lobes and wings of X-shaped sources have specific relationships and are not a random sampling of the morphologies observed in double radio sources. The main lobes are almost always edge-brightened and have bridges extending to the core. The wings do not have hotspots and they too are always extended all the way to the core. It is also difficult to account for the lobe-wing pairing seen in several X-shaped sources and the minor axis preference for the weaker and edge-darkened lobe pair in such a model.

In an alternate model suggested by Leahy & Williams (1984), X-shaped sources might be a result of an axis flip following which backflow from the new lobes rejuvenates the relic lobe maintaining its visibility. In this picture a pre-existing channel along the minor axes as a conduit for the backflowing material might be naturally present as a relic cocoon, if the earlier activity prior to the black-hole merger and associated axis flip were aligned with the host minor axis.

Consistent with the finding that there is no preferred alignment between the radio axis and host optical axis in a general population of radio sources, we might expect all possible orientations of the black hole spin axis prior to a merger and associated flip. Within the black-hole merger model, flips from minor-axis to major-axis result in the new source experiencing enhanced backflow and, consequently a tendency to manifest as an X-shaped radio source if the backflow illuminates the relic lobes closer to the minor axis. The question then arises as to the outcome of axis flips from an initial major-axis state to a minor-axis orientation.

In this context, of relevance is the recent discovery of non-thermal X-ray emission in the high redshift radio galaxy, 3C294, on either side of the core, and at a P.A. offset of about  $50^\circ$  from the main radio axis; the X-ray lobes are not visible in the radio (Erlund et al. 2006). Axis flips from a major- to minor-axis source would be expected to create new lobes along the minor axis, with poor backflow, less likelihood of forming an X-shaped radio source, but would result in a minor-axis double radio source with a relic pair of radio-invisible lobes closer to the major axis that might be visible in its inverse-Compton scattering of cosmic microwave background radiation.

#### 7.4. The role of black-hole axis re-orientation

A final point is regarding our finding of a tendency for giant radio sources to preferentially be oriented closer to the host minor axis. In the unified model presented above seeking a common explanation for the formation of giants, X-shaped radio sources and off-axis lobe distortions, anisotropy in the galaxy environment is offered as the cause. We comment on another aspect here.

If the minor axis in elliptical galaxies represents the axis of the large scale galaxy potential, it is the direction to which an offset black-hole axis may be re-oriented, as a result of an opposing torque to the torque that the black hole exerts on the immediate accretion disk surrounding it in the attempt to position it in its equatorial plane (Natarajan & Pringle 1998). This re-alignment timescale has been estimated to be  $\sim 10^6$  yr, for Eddington accretion rates, but could be larger for lower accretion rates.

The median linear size of radio sources are observed to be larger for orientations closer to the host minor axis (Fig. 2), which might be interpreted as alignment of the radio axis with the host minor axis with age. If this realignment is owing to the above Natarajan & Pringle (1998) model, we may expect that re-alignment timescales are comparable to lifetimes of giant radio galaxies, and that accretion rates are significantly below Eddington. However, since the distribution of radio axes of sources is fairly uniform (Fig. 1), implying that sources with relatively smaller sizes—presumably younger—are major-axis sources, the onset of radio activity is coeval with an event that offsets black hole axes away from the stable minor-axis direction.

## 8. Conclusions

We have presented a new class of X-shaped radio sources, which lack hotspots and are sometimes edge-darkened. Many of this class are observed to have double-double radio source morphologies.

We have explored relations between radio source morphologies and the relative angle between the radio axis and host optical galaxy axes. The study is based entirely on axis orientations as projected on the sky. The well known 3CRR sample of nearby radio galaxies has been used given the high quality radio and optical data available for this sample. Radio-optical morphology relations have been also examined for representative samples of giant radio galaxies and, separately, X-shaped radio sources. The main conclusions of our study are:

(1) Wing formation in both edge-brightened as well as edge-darkened X-shaped radio sources may be understood as arising from redirection of backflow into wings. Most edge-darkened X-shaped radio sources are presently undergoing renewed nuclear activity that is observed in the form of inner double structures: we propose that the wings in edge-darkened X-shaped radio sources represent backflows from a past activity episode.

(2) FR-II type edge-brightened lobes, formed by powerful beams in hot-spot radio sources, may evolve into edge-darkened FR-I type morphology following cessation of jet activity.

(3) Although double radio sources may have axes randomly distributed with respect to the host galaxy axes, the size to which a radio source grows and its radio morphology are influenced by the relative orientation. Minor-axis sources tend to have larger linear sizes compared to major-axis sources. Major-axis sources have a greater propensity for off-axis lobe distortions in the form of winged structures as compared to minor-axis sources.

(4) Giant radio galaxies are preferentially oriented along their host minor axes.

(5) Winged radio galaxies are predominantly major-axis sources.

(6) X-shaped radio sources have radio axes within  $50^\circ$  of their host major axes. The wings in X-shaped radio sources are within  $40^\circ$  of their host minor axes. Although the main radio axes in these sources are fairly uniformly distributed over the range, the wings have a strong preference to be within about  $10^\circ$  of the host minor axes.

(7) In X-shaped radio sources with higher radio power, the wings have a relatively higher propensity to be oriented closer to the host minor axis.

We are led to the conclusion that the morphology of powerful double radio sources depends on whether the source is of major- or minor-axis type. The reason appears to be an anisotropy in the environment, which is related to the ellipticity of the host galaxy. The anisotropy appears to influence the forward advance of the beams, the strength of the backflow in the cocoon, and the formation of wings and off-axis distortions in the lobes. The interaction of backflows in a major-axis radio source with an anisotropic environment associated with the host—perhaps an elliptic halo—appears necessary for the formation of X-shaped radio sources; this may indeed be a sufficient condition.

There is observational evidence for binary nuclei and axis flips in AGNs. Axis flips may not be a necessary or dominant mechanism for the formation of X-shaped radio sources. Nevertheless, the study presented here suggests that even if axis flips are the cause for the formation of X-shaped radio sources, backflows appear to be important in directing material from the new lobe into the relic lobes.

The lack of any preferred radio-optical P.A. for the general population of radio sources suggests that the initial orientation of an active radio source prior to a black-hole merger might not have any preferred direction. Assuming this is so, an interesting outcome is that if X-shaped radio sources are created by axis flips in the black-hole merger model, an equal number of minor-axis radio sources ought to exist, representing sources in which the axis has flipped from a major- to minor-axis orientation, in which the relic lobe along the major axis might be observable in inverse-Compton X-rays and not in radio emission. However, if black holes are re-oriented to align with the host minor axis over time, black-hole mergers and associated axis flips might result in post-merger radio sources that avoid the minor axis.

This publication makes use of data products from the Two Micron All Sky Survey, which is a joint project of the University of Massachusetts and the IPAC/California Institute of Technology, funded by NASA and the NSF. This research has made use of data obtained from the SuperCOSMOS Science Archive, prepared and hosted by the Wide Field Astronomy Unit, IoA, University of Edinburgh, which is funded by the UK PPARC. The Digitized Sky Surveys were produced at the STScI under US Government grant NAG W-2166.

## REFERENCES

- Alexander, P.; Leahy, J. P., 1987, MNRAS 225, 1
- Andreasyan, R. R.; Sol, H., 1999, Astrophysics 42, 275
- Battistini, P.; Bonoli, F.; Silvestro, S.; Fanti, R.; Gioia, I. M.; Giovannini, G., 1980, A&A 42, 357
- Baum, Stefi Alison; Heckman, Timothy M.; Bridle, Alan; van Breugel, Wil J. M.; Miley, George K., 1988, ApJS 68, 643
- Birkinshaw, M.; Davies, R. L., 1985, ApJ 291, 32
- Black, A. R. S.; Baum, S. A.; Leahy, J. P.; Perley, R. A.; Riley, J. M.; Scheuer, P. A. G., 1992, MNRAS 256, 186
- Blundell, K.; Rawlings, S., 2000, AJ 119, 1111
- Capetti, A.; de Ruiter, H. R.; Fanti, R.; Morganti, R.; Parma, P.; Ulrich, M.-H., 2000, A&A 362, 871
- Capetti, A., Zamfir, S., Rossi, P., Bodo, G., Zanni, C., Massaglia, S, 2002, A&A, 394, 39

- Cheung, C. C., AJ 133, 2097
- Cordey, R. A., 1987, MNRAS 227, 695
- Dave, Romeel; Oppenheimer, Benjamin D.; Sivanandam, Suresh, 2008, arXiv:0805.1938
- de Koff, S., et al., 1996, ApJS 107, 621
- de Koff, S., et al., 2001, ApJS 129, 33
- Dennett-Thorpe, J.; Scheuer, P. A. G.; Laing, R. A.; Bridle, A. H.; Pooley, G. G.; Reich, W., 2002, MNRAS 330, 609
- de Vries, W. H.; O’Dea, C. P.; Barthel, P. D.; Fanti, C.; Fanti, R.; Lehnert, M. D., 2000, AJ 120, 2300
- Erlund, M. C.; Fabian, A. C.; Blundell, Katherine M.; Celotti, A.; Crawford, C. S., 2006, MNRAS 371, 29
- Evans, D. A. et al., 2008, ApJ 675, 1057
- Fanaroff, B. L.; Riley, J. M., 1974, MNRAS 167, 31P
- Gibson, D. M., 1975, A&A 39, 377
- Guthrie, B. N. G., 1980, Ap&SS 70, 211
- Hardcastle, M. J., Hardcastle, M. J.; Kraft, R. P.; Worrall, D. M.; Croston, J. H.; Evans, D. A.; Birkinshaw, M.; Murray, S. S. 2007, ApJ 662, 166
- Harvanek, Michael; Hardcastle, Martin J., 1998, ApJS 119, 25
- Jaegers, W. J., 1987, A&AS 71, 603
- Jones, Paul A.; McAdam, W. B., 1992, ApJS 80, 137
- Junor, W.; Mantovani, F.; Morganti, R.; Padrielli, L., 2000, A&AS 143, 457
- Keel, William C.; Martini, Paul, 1995, AJ 109, 2305
- Kraft, R. P.; Hardcastle, M. J.; Worrall, D. M.; Murray, S. S., 2005, ApJ 622, 149
- Laing, R. A.; Riley, J. M.; Longair, M. S., 1983, MNRAS 204, 151
- Lal, D. V.; Rao, A. P., 2007, MNRAS 374, 1085

- Landt, Hermine; Perlman, Eric S.; Padovani, Paolo, 2006, ApJ 637, 183
- Leahy, J. P.; Williams, A. G., 1984, MNRAS 210, 929
- Leahy, J. P.; Perley, R. A., 1991, AJ 102, 537
- Leahy, J. P.; Parma, P., 1992, Extragalactic Radio Sources. From Beams to Jets. Eds.: J. Roland, H. Sol, G. Pelletier, Cambridge University Press, 1992., p. 307
- Leahy, J. P.; Black, A. R. S.; Dennett-Thorpe, J.; Hardcastle, M. J.; Komissarov, S.; Perley, R. A.; Riley, J. M.; Scheuer, P. A. G., 1997, MNRAS 291, 20
- Ledlow, Michael J.; Owen, Frazer N., 1995, AJ 110, 1959
- Lehar, J.; Buchalter, A.; McMahon, R. G.; Kochanek, C. S.; Muxlow, T. W. B., 2001, ApJ 547, 60
- Liu, F. K., 2004, MNRAS 347, 1357
- Mack, K.-H.; Gregorini, L.; Parma, P.; Klein, U., 1994, A&AS 103, 157
- Macklin, J. T., 1983, MNRAS, 203, 145
- Madrid, Juan P. et al., 2006, ApJS, 164, 307
- Martel, Andre R. et al., 1999, ApJS 122, 81
- McCarthy, Patrick J.; van Breugel, Wil; Kapahi, Vijay K., 1991, ApJ 371, 478
- McCarthy, Patrick J.; Spinrad, Hyron; van Breugel, Wil, 1995, ApJS 99, 27
- McLure, R. J.; Kukula, M. J.; Dunlop, J. S.; Baum, S. A.; O’Dea, C. P.; Hughes, D. H., 1999, MNRAS 308, 377
- Merritt, D.; Ekers, R. D., 2002, Science 297, 1310
- Morganti, R.; Tadhunter, C. N.; Oosterloo, T. A., 2005, A&A 444, 9
- Murgia, M.; Parma, P.; de Ruiter, H. R.; Bondi, M.; Ekers, R. D.; Fanti, R.; Fomalont, E. B., 2001, A&A 380, 102
- Natarajan, Priyamvada; Pringle, J. E., 1988, ApJ 506, 97
- Owen, Frazer N.; Ledlow, Michael J., 1997, ApJS 108, 41
- Palimaka, J. J.; Bridle, A. H.; Brandie, G. W.; Fomalont, E. B., 1979, ApJ 231, 7

- Roche, Nathan; Eales, Stephen A., 2000, MNRAS 317, 120
- Roettiger, K.; Burns, J. O.; Clarke, D. A.; Christiansen, W. A., 1994, ApJ Letters, 421, 23
- Safouris, V.; Subrahmanyan, R.; Bicknell, G. V.; Saripalli, L., 2008, MNRAS 385, 2117
- Sansom, A. E., et al. 1987, MNRAS 229, 15
- Saripalli, L.; Gopal-Krishna; Reich, W.; Kuehr, H., 1986, A&A 170, 20
- Saripalli, Lakshmi; Subrahmanyan, Ravi; Udaya Shankar, N., 2002, ApJ 565, 256
- Saripalli, Lakshmi; Subrahmanyan, Ravi; Udaya Shankar, N., 2003, ApJ 590, 181
- Saripalli, L.; Hunstead, R. W.; Subrahmanyan, R.; Boyce, E., 2005, AJ 130, 896
- Saripalli, Lakshmi; Subrahmanyan, Ravi; Laskar, Tanmoy; Koekemoer, Anton, 2008, Proceedings of Science (MRU) 052, 130, From planets to dark energy: The modern radio universe, University of Manchester, Manchester, UK, 1–5 October, 2007
- Saikia, D. J.; Konar, C.; Kulkarni, V. K., 2006, MNRAS 370, 80
- Schoenmakers, Arno P.; de Bruyn, A. G.; Röttgering, H. J. A.; van der Laan, H., 2000, MNRAS 315, 395
- Spangler, S. R.; Sakurai, T., 1985, ApJ 297, 84
- Springmann, Alessandra and Cheung, Chi, 2007, Journal of Undergraduate Research 7, 97
- Subrahmanyan, R.; Saripalli, L.; Hunstead, R. W., 1996, MNRAS 279, 257
- Subrahmanyan, R.; Saripalli, L.; Safouris, V.; Hunstead, R. W., 2008, ApJ 677, 63
- Sullivan, W. T., III; Sinn, L. A., ApL 16, 173
- Ulrich, M.-H.; Roenback, J., 1996, A&A 313, 750
- Veilleux, Sylvain; Cecil, Gerald; Bland-Hawthorn, Joss, 2005, ARA&A 43, 769
- Wang, T. G., Zhou, H. Y., Dong, X. B., 2003, AJ 126, 113
- Zakamska, Nadia L.; Strauss, Michael A.; Heckman, Timothy M.; Ivezia, Aeljko; Krolik, Julian H., 2004, AJ 128, 1002
- Zhang, Xue-Guang; Dultzin-Hacyan, D.; Wang, Ting-Gui, 2007, MNRAS 377, 1215

Zier, C., Biermann, P. L., 2001, *A&A*, 377, 23

Table 1. The 3CRR sample

Name	Redshift	FR class	PA-Radio	PA-Optical	$\Delta$ PA	ellipticity	Reference
3C16	0.405	II	28.8	-22*	50.8	0.28*	deV 2000
3C19	0.482	II	29.3	***		0	deV 2000
3C20	0.174	II	103.13	130	26.87	0.28	deK 1996
3C28	0.1971	II	149.7	155	5.3	0.39	deK 1996
3C31	0.0173	I	162*	144	18	0.12	Mar 1999
3C33.1	0.181	II	44.5	63	18.5	0.26	deK 1996
3C33	0.0595	II	19.2	148*	51.2	0.26*	Bau 1988
3C35	0.067	II	9.6	111	78.6	0.26	Mar 1999
3C42	0.395	II	131.6	153	21.4	0.47	deK 1996
3C46	0.4373	II	65	***		0	deV 2000
3C61.1	0.186	II	2.1	165	17.1	0.18	deK 1996
3C66B	0.0215	I	45*	135	90	0.05	Mar 1999
3C67	0.3102	II	175.3	175	0.3	0.4	deK 1996
3C76.1	0.0324	I	139	140*	1	0.12*	MAST
3C79	0.2559	II	101	25*	76	0.16*	MAST
3C83.1	0.0179	I	100	166	66	0.22	Mar 1999
3C98	0.0306	II	21	55	34	0.13	Mar 1999
3C109	0.3056	II	151	***		0	Bau 1988
3C123	0.2177	II	114.9	90	24.9	0.32	deK 1996
3C132	0.214	II	130.8	7	56.2	0.25	deK 1996
3C153	0.2769	II	48	125*	77	0.21*	MAST
3C171	0.2384	II*	100.9	***		0	MAST
3C173.1	0.292	II	18.5	8	10.5	0.23	deK 1996

Table 1—Continued

Name	Redshift	FR class	PA-Radio	PA-Optical	$\Delta$ PA	ellipticity	Reference
3C184.1	0.1182	II	161.8	40	58.2	0.18	deK 1996
3C192	0.0598	II	123.3	***		0	Mad 2006
3C200	0.458	II	155.3	150	5.3	0.36	deK 1996
3C219	0.1744	II	39.6	145	74.6	0.08	deK 1996
3C223	0.1368	II	163.2	75*	88.2	0.1*	Mad 2006
3C234	0.1848	II	62	***		0	McL 1999
3C236	0.0989	II	122.8	44	78.8	0.44	Mar 1999
3C244.1	0.428	II	168	76	88	0.2	deK 1996
3C268.3	0.371	II	160.6	144	16.6	0.46	deK 1996
3C272.1	0.004	I	0	126	54	0.17	Mar 1999
3C274	0.004	I	114	0.3	66.3	0.03	Mar 1999
3C274.1	0.422	II	75.5	***		0	deK 1996
3C284	0.2394	II	101.4	42*	59.4	0.19*	MAST
3C285	0.0794	II	82.8	129*	46.2	0.55*	MAST
3C288	0.246	II*	141	***		0	deK 1996
3C293	0.04503	II	128.1	66	62.1	0.54	Mar 1999
3C295	0.4599	II	144.3	***		***	Bau 1988
3C296	0.0237	I	36.5	148	68.5	0.21	Mar 1999
3C299	0.367	II	63.6	47	16.6	***	deK 1996
3C300	0.27	II	126.7	104	22.7	0.47	Roc 2000
3C303	0.141	II	98.6	0.0*	81.4	0.1*	deK 1996
3C305	0.041	II*	44.2	76	31.8	0.37	Mar 1999
3C310	0.054	II	160.9*	86	74.9	0.18	Mar 1999

Table 1—Continued

Name	Redshift	FR class	PA-Radio	PA-Optical	$\Delta$ PA	ellipticity	Reference
3C314.1	0.1197	I	144*	75	69	0.31	deK 1996
3C315	0.1083	I	8.4	33	24.6	0.46	deK 1996
3C319	0.192	II	43.5	146	77.5	0.17	Roc 2000
3C321	0.096	II	134.7	***		***	Mar 1999
3C326	0.0885	II	78.3	150*	71.7	0.5*	Roc 2000
3C341	0.448	II	53.4	***		0	Roc 2000
3C346	0.161	II*	72.6	122	49.4	0.23	deK 1996
3C349	0.205	II	146	14	48	0.31	deK 1996
3C381	0.1605	II	3.5	58*	54.5	0.18*	MAST
3C382	0.0578	II	51	85	34	0.22	Mar 1999
3C386	0.017	I	14*	102	88	0.13	Mar 1999
3C388	0.0908	II	61.3	40	21.3	0.13	Mar 1999
3C390.3	0.0569	II	149	82	67	0.16	Mar 1999
3C401	0.201	II	16	0.3	15.7	0.123	Roc 2000
3C433	0.1016	II*	164.5	145*	19.5	0.47*	deK 1996, MAST
3C436	0.2145	II	176.4	3	6.6	0.31	deK 1996
3C438	0.29	II	128.4	***		***	MAST
3C442A	0.0263	II	64*	131	67	0.13	Mar 1999
3C449	0.0171	I	10*	1	9	0.2	Mar 1999
3C452	0.0811	II	75	101	26	0.32	Mar 1999
3C457	0.428	II	40	***		***	***
3C465	0.0313	I	123.2	30	86.8	0.22	Mar 1999
4C12.03	0.157	II	22.63	160	42.63	0.32	2MASS

Table 1—Continued

Name	Redshift	FR class	PA-Radio	PA-Optical	$\Delta$ PA	ellipticity	Reference
4C14.11	0.206	II	140	***		***	***
4C14.27	0.392	II	107.5	***		***	***
4C73.08	0.0581	II	70	25	45	0.26	2MASS
DA240	0.035	II	61.23	40	21.23	0.14	2MASS
NGC6251	0.024	I	111	30	81	0.1	2MASS

\*For optical: quoted value either differs from the value in deK96 or is not present in deK96. Used MAST FITs data for 3C76.1, 3C79, 3C153, 3C284, 3C285 and 3C381. For others, values were measurements based on data in references cited. For radio: P.A. of jets were measured from higher resolution images or from central regions in the case of relaxed doubles.

\*\*\*Indeterminate either because the object is confused or there is lack of relevant data in literature

References. — Bau1988—Baum et al. 1988; deK1996—de Koff et al. 1996; Mar1999—Martel et al. 1999; Roc2000—Roche & Eales 2000; deV2000—de Vries et al. 2000; Mad2006—Madrid et al. 2006; McL1999—McLure et al. 1999; MAST—Multimission Archives at STScI

Table 2. Radio-optical data for giant radio galaxies from Schoenmakers et al. (2000) (z<sub>j</sub>0.15) and Subrahmanyam et al. (1996) with good optical images

IAU-Name	Redshift	FR class	PA-Radio	PA-Optical	ΔPA	Reference
B0055+300 (NGC315)	0.0167	I	135	55	80	2MASS
B0109+492 (3C35)	0.067	II	9.6	111	78.6	Mar 1999
B0157+405 (4C40.08)	0.0827	II?	109	66	43	DSS
B0309+411	0.134	II	130	47	83	DSS
B0648+733	0.1145	II	52	-40	88	2MASS
B0745+560 (DA240)	0.035	II	61.23	40	21.23	2MASS
B0945+734 (4C73.08)	0.0581	II	70	25	45	2MASS
B1003+351 (3C236)	0.0989	II	122.8	44	78.8	Mar 1999
B1209+745 (4CT74.17.1)	0.107	I	154	53	79	2MASS
B1309+412	0.1103	II	6	***		2MASS
B1312+698 (DA340)	0.106	II	127	11	64	DSS
B1426+295	0.087	II	45	-35	80	DSS
B1626+518	0.0547	II	35	-65	80	2MASS
B1637+826 (NGC6251)	0.024	I	111	30	81	2MASS
B0114-476	0.146	II	172	7	15	SuperCOSMOS
B0211-479	0.2195	II	173	145	28	SuperCOSMOS
B0511-305	0.0583	II		***		SuperCOSMOS
B1545-321	0.1085	II		***		SuperCOSMOS

\*\*\*Indeterminate because optical image appears circular

Table 3. The X-shaped source sample

Name	Redshift	FR class	LLS (kpc)	$P_{1.4}$ (W/Hz)	PA-Radio (deg.)	PA-Wing (deg.)	PA-Optical (deg.)	ellipticity	W/M	Ref Optical	Ref Radio
4C12.03	0.156	II	623	26.11	22.6	65	160	0.32	1.06	2MASS	Lea 1991
B0037+209 (Abell 75)	0.0622	II	189	24.05	119	40	85	0.456	0.57	DSS Led 1995	Owe 1997
3C20	0.174	II	155.2	26.34	103.13	17	130	0.28	0.72	deK 1996	3CRR atlas
NGC326	0.047	II	112.6	24.95	135	55	***	0	2.13	Cap 2000	Mur 2001
J0116-473	0.146	II	1896	26.21	170	70	2	0.21	0.76	DSS	Sar 2002
3C52	0.2854	II	329	26.99	22	114	20	0.36	0.88	deK 1996	Lea 1984
3C63	0.175	II	84.7	26.47	34	130	79	0.26	1.53	deK 1996	Har 1998
3C76.1	0.0324	I	128	24.7	139	57	140*	0.12*	0.87	MAST	3CRR atlas
3C136.1	0.064	II	543.1	25.47	107	0	117	0.39	0.97	Mar 1999	Lea 1984
3C192	0.0598	II	229	25.63	123.3	35	***	0	0.66	Mad 2006	Bau 1988
3C197.1 (Abell 646)	0.1303	II	47	25.79	0	71	***	0	1	deK 1996	Owe 1997
4C32.25	0.0512	II	338	25.06	64	0	84	0.15	0.83	Ulr 1996	Mac 1994
3C223.1	0.1074	II	163.4	25.77	15	130	40	0.45	1.4	deK 1996	Bla 1992
4C48.29	0.052	II	459	25.03	170	105	***	0	1	DSS	Jag 1987
J1101+167 (Abell 1145)	0.0677	II	270	24.84	114	20	64	0.291	1.42	DSS Led 1995	Owe 1997
4C01.30	0.1324	II	116	25.49	100	24	85	0.3	1.97	Wan 2003	Wan 2003
B1142+157 (Abell 1371)	0.067	II	45	24.48	59	153	67	0.329	0.87	DSS Led 1995	Owe 1997
4C04.40 (B1203+043)		II			35	136			1.12	—	Jun 2000
J1210+719 (Abell 1484)	0.1226	I	110	24.99	162	74	125	0.476	0.92	DSS Led 1995	Owe 1997
J1357+4807	0.383	II	57.5	26.16	18	65			1.28	—	Leh 2001
3C315	0.1083	I	394	26.1	8.4	123	33	0.46	0.93	deK 1996	Lea 1984
J1534+103	0.1333	I	524	25.13	171	72	***	0	0.57	DSS	Owe 1997

Table 3—Continued

Name	Redshift	FR class	LLS (kpc)	$P_{1.4}$ (W/Hz)	PA-Radio (deg.)	PA-Wing (deg.)	PA-Optical (deg.)	elipticity	W/M	Ref Optical	Ref Radio
(Abell 2091)											
3C379.1	0.256	II	340	26.57	161	45	***	0	0.63	deK 1996	Spa 1985
3C401	0.201	II	78.4	26.5	16	109	0.3	0.123	0.78	Roc 2000	3CRR atlas
3C403	0.059	II	129	25.68	79	135	39	0.25	2	Mar 1999	Bla 1992
B2014-55	0.06	I	1513	25.18	155	72	10	0.4	0.57	DSS	Jon 1992
3C433	0.1016	II*	127	26.48	164.5	60	145*	0.47*	0.88	deK 1996	3CRR atlas
										MAST	
3C438	0.29	II	100	27.2	128.4	40	***	***	0.68	MAST	3CRR atlas
J2157+0037	0.3907	II	427.5	26.11	69	151			1.22	—	Zak 2004
J2347+0852	0.292	II	314.4	25.62	135	52	148	0.15	1.38	DSS	Lan 2006
B2356-611	0.0963	II	736	26.68	133	90	3	0.37	0.91	DSS	Sub 1996

\*\*\*:indeterminate or optical image appears circular

References. — For Optical: Cap 2000—Capetti et al. 2000; deK1996—de Koff et al. 1996; Led 1995—Ledlow & Owen 1995; Mad 2006—Madrid et al. 2006; Mar 1999—Martel et al. 1999; MAST—Multimission Archives of STScI; Roc 2000—Roche & Eales 2000; Ulr 1996—Ulrich & Roenback 1996; Wan 2003—Wang, Zhou & Dong 2003; For Radio: Bau 1988—Baum et al. 1988; Bla 1992—Black et al. 1992; Jag 1987—Jaegers 1987; Jon 1992—Jones & McAdam 1992; Jun 2000—Junor et al. 2000; Lan 2006—Landt, Perlman & Padovani 2006; Lea 1984—Leahy & Williams 1984; Lea 1991—Leahy & Perley 1991; Leh 2001—Lehar et al. 2001; Mac 1994—Mack et al. 1994; Mur 2001—Murgia et al. 2001; Owe 1997—Owen & Ledlow 1997; Sar 2002—Saripalli, Subrahmanyan & Udaya Shankar 2002; Spa 1985—Spangler & Sakurai 1985; Sub 1996—Subrahmanyan, Saripalli & Hunstead 1996; Zak 2004—Zakamska et al. 2004

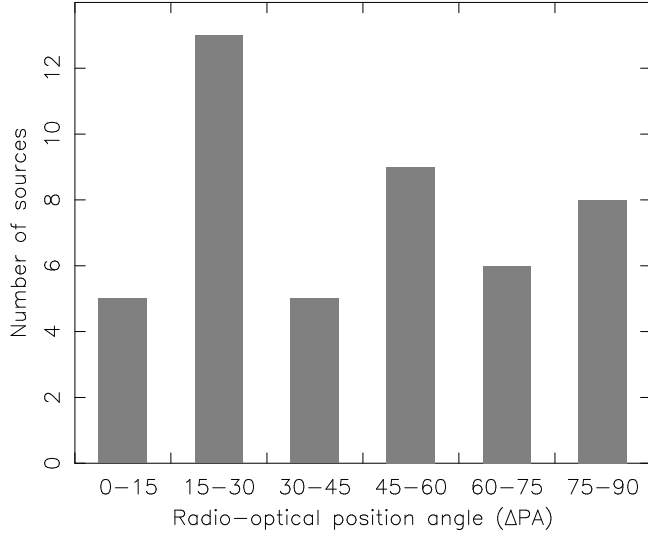


Fig. 1.— Histogram of  $\Delta PA$  for the 3CRR FR-II sources.

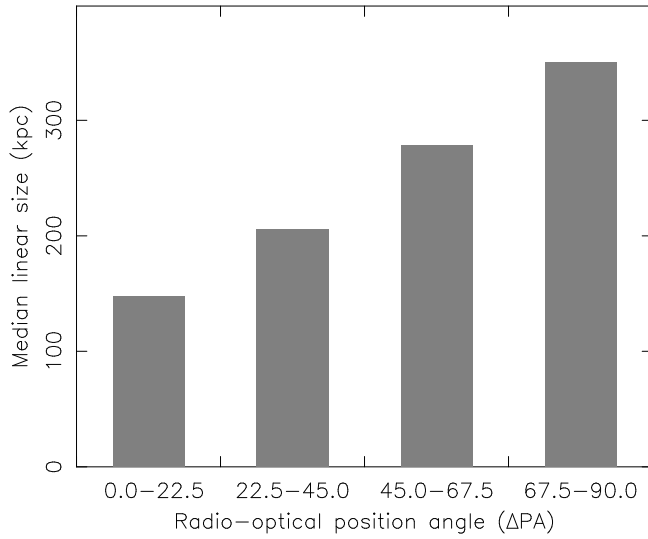


Fig. 2.— Bar graph of the median projected linear size, in kpc, for the 3CRR FR-II radio sources binned in intervals of  $\Delta PA$ .

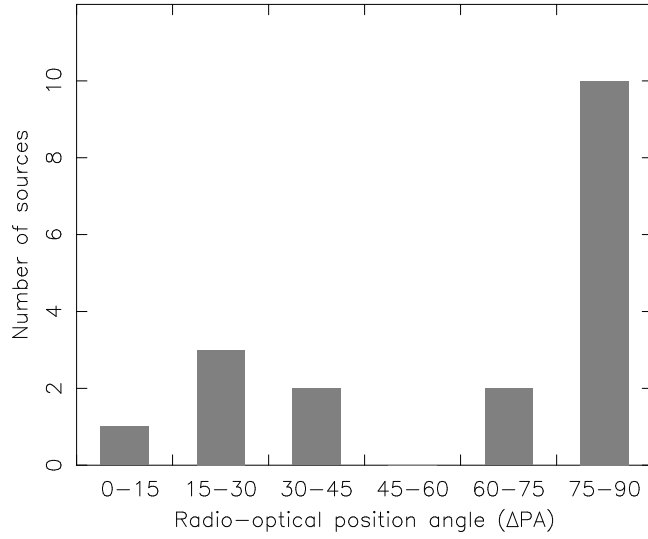


Fig. 3.— Histogram of  $\Delta PA$  for the giant radio sources.

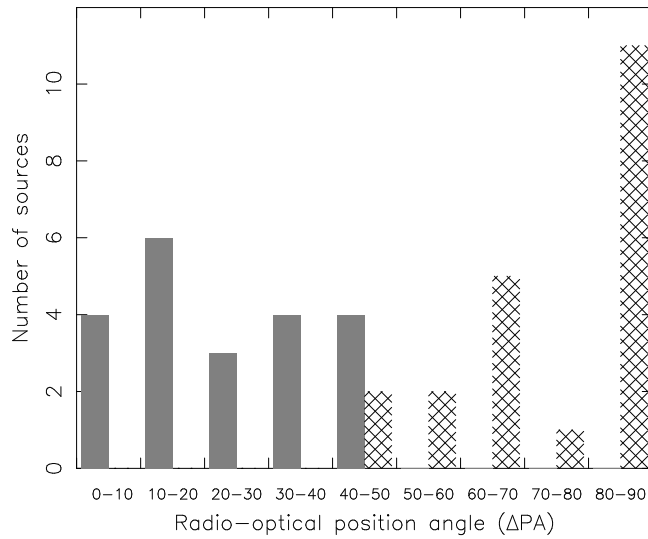


Fig. 4.— Histogram of  $\Delta PA$  for the X-shaped radio sources: the  $\Delta PA$  distribution for the main source axis is shown using shaded bars and the  $\Delta PA$  for the wings is shown as cross-hatched bars.

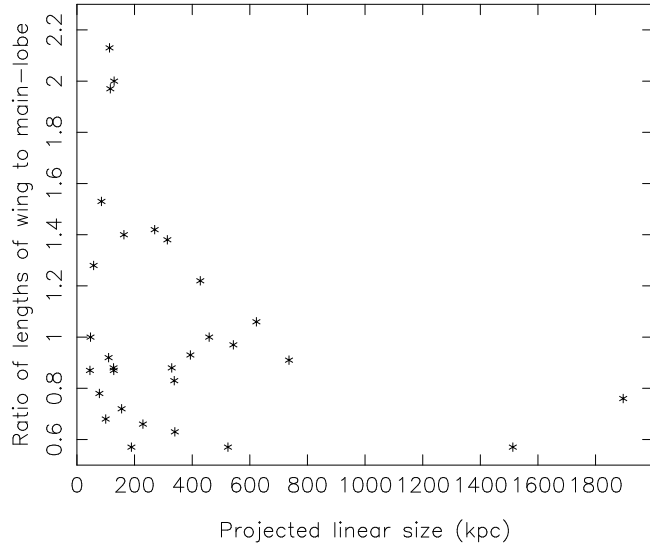


Fig. 5.— Plot of the ratio of projected lengths of wings to main lobes, for the sample of X-shaped radio sources, versus the projected linear size.

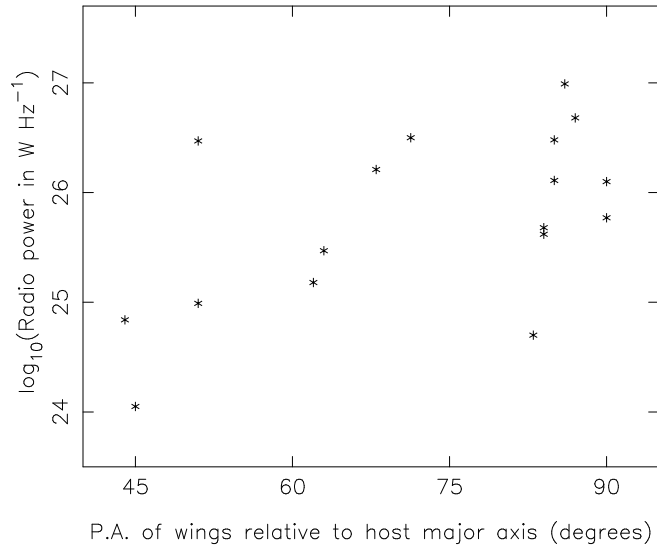


Fig. 6.— Plot of the radio power of the X-shaped radio sources versus the position angle of the wings relative to the major axis of the host.

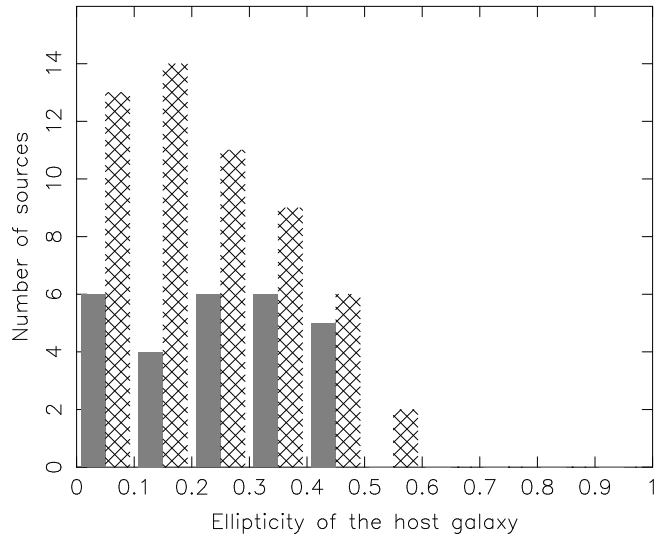


Fig. 7.— Histogram of ellipticities of the host galaxies for the X-shaped radio sources compared with that for hosts of 3CRR FR-II sources. The bars for the X-shaped radio sources is shown using shaded bars and that for the 3CRR FR-II hosts is shown as cross-hatched bars.